forum acusticum 2023

EXPERIMENTAL VALIDATION OF THE LENGTH CORRECTION FACTOR FOR FOLDED QUARTER-WAVELENGTH RESONATORS

F. De Bie[1,3*] **H. Denayer**[2,3] **C. Claeys**[2,3]
E. Deckers[1,3]
[1] Department of Mechanical Engineering campus Diepenbeek, KU Leuven, Belgium
[2] Department of Mechanical Engineering campus Heverlee, KU Leuven, Belgium
[3] Flanders Make@KU Leuven, Belgium

ABSTRACT

Quarter-wavelength acoustic metamaterials consist of multiple quarter wavelength resonators that are tuned to different resonance frequencies to create broadband sound absorption. To maintain a compact volume at low frequencies, these resonators are often folded. The impact of a fold on the resonance frequency of a quarter-wavelength resonator has been investigated numerically in a previous study [1] and a length correction factor to account for these effects was also proposed. In this paper, the validity of this correction factor is assessed experimentally. To this end, several test samples are 3D printed using an FDM printer. Each sample consists of quarter-wavelength resonators with a single 90° bend and a resonance frequency between 1000 Hz and 2000 Hz. The absorption coefficient of each sample is measured in an impedance tube according to the ISO 10534-2 standard. The experimental results are then compared to the model. It is found that the analytical and experimental results show good agreement, which implies that the use of the proposed correction factor is justified.

Keywords: *acoustic metamaterials, quarter-wavelength resonator, length correction, experimental validation*

1. INTRODUCTION

Acoustic quarter-wavelength metamaterials are a broadband and space-efficient solution to low-frequency noise problems [2-6]. These metamaterials consist of a number of (optimized) quarter-wavelength resonators, each tuned to a different frequency and arranged in parallel and/or series. To maintain a compact volume, the resonators can be coiled up or folded, as shown in [2-5], or a side-branch configuration can be used, as presented in [6]. In this paper, only folded quarter-wavelength resonators are discussed.

In a previous study [7], it was shown that the effect of folding on a resonator's resonance frequency can be significant. In said study, the effective length of a folded resonator was set to equal the centerline length, which led to inaccurate predictions. An alternative approach is discussed in [4], where the effective length of a folded resonator is calculated using Pythagorean's theorem. Although this approach leads to accurate results for labyrinth-like structures, its applicability for arbitrary folded resonators is less straightforward. Therefore, a more general expression to account for the effect of a 90° fold on the effective length of a resonator was presented in [1].

In the present paper, the use of this semi-analytical expression is experimentally validated for resonators with a square (3 x 3 mm²) and rectangular (5 x 3 mm²) cross-section. The repeatability of the 3D printing process is also preliminary assessed.

[*] ***Corresponding author***: femke.debie@kuleuven.be

2. MODEL DESCRIPTION

The absorption coefficient α (unit: /) of a quarter-wavelength metamaterial can be calculated using **Eqn.(1)** [8]:

$$\alpha = 1 - \left|\frac{Z_t - Z_0}{Z_t + Z_0}\right|^2. \quad (1)$$

Herein, Z_0 represents the characteristic impedance of the medium (unit: Pa.s/m), which equals $\rho_0 c_0$ with ρ_0 the ambient density (unit: kg/m³) and c_0 the ambient speed of sound (unit: m/s).
The frequency (unit: Hz) corresponding to the maximum α-value will later be referred to as the resonance frequency of the resonator. Z_t is the surface impedance of the acoustic metamaterial (unit: Pa.s/m). For a parallel arrangement consisting of i resonators and with no interaction effects considered, Z_t can be calculated using **Eqn.(2),** which is based on the acoustics-electrics analogy:

$$Z_t = \left[\sum_{i=1}^{i=n} \frac{1}{Z_i}\right]^{-1}. \quad (2)$$

Z_i denotes the surface impedance of a single quarter-wavelength resonator in which thermal-viscous losses occur (unit: Pa.s/m). This impedance can be determined using **Eqn.(3)** [8-12]:

$$Z_i = -j\frac{1}{\phi_i}\tilde{Z}_i \cot\left(\tilde{k}_i L_{\text{eff},i}\right) + j\frac{1}{\phi_i}\rho_0 \omega \varepsilon_i. \quad (3)$$

In Eqn. (3), $\tilde{Z}_i$ and $\tilde{k}_i$ are, respectively, the dynamic impedance (unit: Pa.s/m) and dynamic wavenumber (unit: m^{-1}) of the equivalent fluid [8]. ϕ_i represents the porosity (unit: /), ω is the angular wave speed (unit: rad/s) and ε_i is the so-called end correction to account for 3D effects at the resonator opening (unit: m). Expressions for ε can be found in [11-12]. $L_{\text{eff},i}$ is the effective length of the resonator (unit: m), which can be calculated using **Eqn.(4)**:

$$L_{\text{eff},i} = L_{\text{CL},i} + \delta_i. \quad (4)$$

L_{CL} symbolizes the centerline length (unit: m) and δ_i is a length correction (unit: m), which accounts for the change in effective length due to folding. In [1], an expression for δ was derived based on numerical simulations. Recently, this expression and its coefficients have been updated to extend the validity up to 2000 Hz and to account for the observed minor dependency of the effective length on the resonator width b (unit: m). The updated expression for δ is given by **Eqn.(5)**:

$$\delta = b\, \mathcal{M}\left(\frac{x}{L_{\text{CL}}}\right) \mathcal{F}\left(\frac{b}{b_{\text{ref}}}\right). \quad (5)$$

With x the distance from the resonator opening to the center of the fold and b_{ref} the reference resonator width. $\mathcal{M}$ is a third-order polynomial given by Eqn.(5a), $\mathcal{F}$ is a second-order polynomial given by Eqn.(5b):

$$\mathcal{M} = -0.722\xi^3 + 1.069\xi^2 + 0.131\xi - 0.478 \quad (5a)$$

$$\mathcal{F} = 0.181\tau^2 - 0.301\tau + 1.120\,. \quad (5b)$$

The ratios x/L_{CL} and b/b_{ref} are further denoted as ξ and τ, respectively. The reference resonator width was set to 6 mm, which corresponds to the maximum value of b within the data pool used to derive Eqn.(5)-(5b).
The length correction factor δ has been verified numerically for a wide range of resonators with a rectangular cross-section that have one 90° bend, a centerline length of at least 0.041 m, a ξ-value between 0.1 and 1 and a height-width ratio between 0.6 and 1.25 (with $b \leq 6$ mm). It was seen that, when using Eqn.(5)-(5b), the resonance frequency of such resonators can be predicted very accurately: the relative deviation between the analytical and numerical prediction is always smaller than 0.25%. An overview of the results of the verification process can be found in **Fig. 1**.

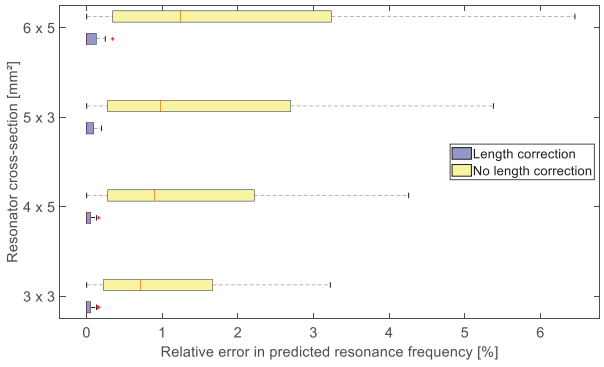

Figure 1. Boxplots showing the relative error between the numerical and analytical model, with and without integration of Eqn.(5)-(5b).

3. TEST MATRIX

An overview of the samples used to validate Eqn.(5)-(5b) under real-life conditions can be found in **Tab. 1**. The selected lengths, cross-sections and ξ-values fall within the validity range of Eqn. (5)-(5b). The bend location and dimensions of the samples (i.e. cross-section and centerline length) are such that the effect of folding should be clearly noticeable. To ensure high absorption, the samples consist of multiple resonators: samples A-D each count eight resonators in parallel, while samples E-F all consist of four resonators in parallel.

Table 1. Ideal dimensions and ξ-values of the eight 3D printed samples

Sample letter	Cross-section dimensions	Centerline length	ξ-value
A	3 x 3 mm²	0.086 m	1
B	3 x 3 mm²	0.086 m	0.15
C	3 x 3 mm²	0.041 m	1
D	3 x 3 mm²	0.041 m	0.5
E	5 x 3 mm²	0.057 m	1
F	5 x 3 mm²	0.057 m	0.15
G	5 x 3 mm²	0.057 m	0.5
H	5 x 3 mm²	0.057 m	0.8

The samples were 3D-printed with an Ultimaker S3, which is a desktop printer with a maximum build volume of 23 x 19 x 20 cm³. The samples are made of PLA and the printer settings were set to 'Engineering', which leads to the highest dimensional accuracy achievable with this system [13]. The printer is located in a climate-conditioned lab to avoid additional temperature variability.

4. EXPERIMENTAL VALIDATION

4.1 Test set-up

The eight samples are all tested in an impedance tube according to the ISO 10534-2 standard. The tube has a diameter of 4 cm. The distance between the two microphones is 34 mm, which sets the lower frequency limit to 500 Hz. Since it concerns resonator arrays, the minimal distance between the sample and the nearest microphone is at least one time the tube's diameter. As the resonators are designed to realize high absorption at one single frequency (instead of the general broadband behavior of porous materials), there will only be one clear absorption peak. Off-resonance, the sample will present only minimal absorption. Hence, only the absorption behavior within a small region around the expected resonance frequency will be discussed.

4.2 Repeatability of the test procedure

Before starting the experimental validation, the repeatability of the entire mounting and test procedure when measuring the absorption coefficient of narrowband structures has to be determined. To this end, one sample out of Table 1 is selected. As the conclusions for this sample should be representative for all other samples in the test matrix, sample G was chosen as it has an average length (0.057 m) and ξ-value (0.5). This sample was repeatedly (re)mounted to the impedance tube and each time, the absorption coefficient was measured. The ambient air temperature during the tests was 20.3 °C, the ambient air pressure 1 bar.

The repeatability of the impedance tube measurements can be evaluated using the repeatability coefficient κ. This coefficient is defined as the value under which the absolute difference between two repetitions will lie and this with a 95 % probability. Otherwise stated: there is a 95 % probability that the absolute difference between two repeated measurements will be smaller than κ.

The repeatability coefficient can be calculated using **Eqn.(6)** [14]:

$$\kappa = 1.96\sqrt{2\sigma^2}. \tag{6}$$

In Eqn.(6), σ^2 represents the variance. After eight test runs, the repeatability coefficient κ was found to be 3.7 Hz.

4.3 Repeatability of the 3D printing process

To assess the repeatability of the 3D printing process, one resonator sample was printed four consecutive times, without recalibrating the printer or changing the printer settings and material. To save printing time, it was opted to print a sample with four unfolded 5 x 3 mm² resonators, which are each 0.041 m long. Under the given ambient conditions, the analytical resonance frequency of the samples is 1993 Hz. The experimental results are shown in **Fig. 2**.

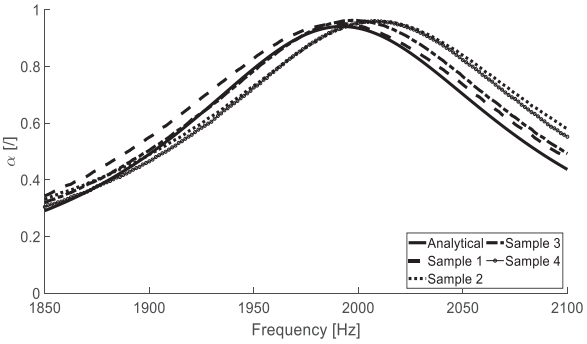

Figure 2. Absorption curves of the four samples used to determine the reproducibility of the 3D printing process. The analytical result serves as reference.

When looking at Fig. 2, it is seen that the resonance frequencies of sample 1 (1989 Hz) and sample 3 (1998 Hz) are close to the analytical prediction of 1993 Hz, while the value for sample 2 (2011 Hz) and 4 (2008 Hz) is more off. In an attempt to explain these differences, the samples were put under a microscope to study the surface of each resonator in more detail. These microscopic images are combined in **Fig. 3**. In this figure, each column represents a different sample (the first column contains the images of sample 1 etc.) and each row corresponds to a different resonator of that sample. The scale of the microscopic images is 0.25 mm/division.

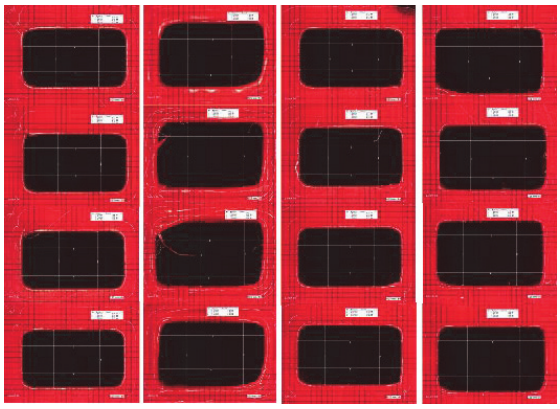

Figure 3. Microscopic images of the surfaces of the four test samples.

When looking at Fig. 3, two statements regarding the 3D-printed resonators can be made:

1. Neither resonator has a perfect rectangular shape: all external corners are rounded. Edge rounding is inherent to FDM printed parts due to the round shape of the nozzle opening.
2. The actual resonators measure under 5 mm x 3 mm at their widest points. The average relative dimensional inaccuracy was largest for sample 1 (8.3 %) and smallest for sample 4 (0.08 %).

In addition to a microscopic study, the overall print quality was assessed by means of a visual inspection. It was seen that the surface quality is lowest for sample 2, which also shows the highest deviation. It was also noticed that one resonator of sample 4 is partially clogged.

In sum, it is clear that the overall print quality (i.e. surface quality and dimensional accuracy) of 3D printed products can substantially vary, even when the same printer settings are used. Hence, an inspection of both the surface and insides of the eventual geometry is highly encouraged. In addition, it can be said that the overall print quality affects the absorption behavior of the metamaterial.

As the goal of this paper is to validate the use of Eqn.(5)-(5b), it is important that dimensional inaccuracies and corner rounding are accounted for such that the analytical results are representative. To this end, each sample is put under a microscope such that the average cross-section dimensions $\bar{b}$ and $\bar{h}$ (unit: m) can be determined for each resonator within the sample. Here, it should be noted that the values of $\bar{b}$ and $\bar{h}$ are assumed to be constant over depth, which might not be the case in reality. In addition, the actual centerline length L' (unit: m) of each resonator is measured using a digital caliper:

- The 5 x 3 mm² resonators are cut open and direct depth measurements are performed;
- For the 3 x 3 mm² resonators, L' is estimated out of the outer dimensions and $\bar{b}$ as the cross-section is too small to fit the depth rod of the caliper.

These actual dimensions ($\bar{b}, \bar{h}$ and L') are then put into the analytical model and a corrected resonance frequency is calculated for each sample using Eqn.(1)-(5b). The corrected resonance frequency will serve as benchmark for the experimental results.

4.4 Validation of the length correction factor δ

4.4.1 Justification of the proposed length correction factor

Fig. 4 gives an overview of the experimental results for the entire test matrix. Fig. 4a-4b show the measured absorption coefficient of samples A-B and C-D, respectively. Fig. 4c displays the measurement data corresponding to samples E-H (see Tab. 1).

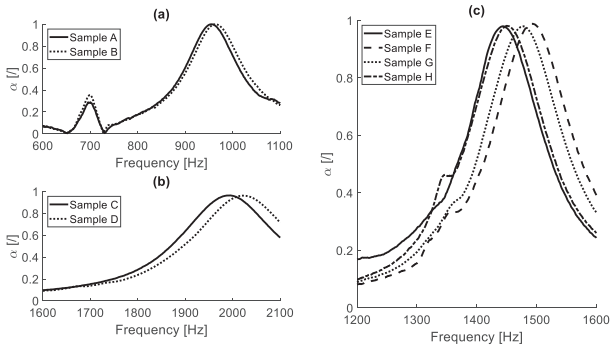

Figure 4. Experimental results for all samples within the test matrix (Tab .1)

Based on Fig.4, several conclusions regarding the relation between δ and the perceived effect of folding on the resonance frequency can be drawn.

Firstly, the resonance frequency of a folded resonator is always higher than the resonance frequency of an unfolded resonator with the same centerline length. Eqn.(5)-(5b) manage to capture this trend, as the value of δ is always negative and leads to a shorter effective length.

Secondly, it can be said that the eventual shift in resonance frequency due to folding (denoted as Δf, unit: Hz) depends on the centerline length. This can be illustrated by looking at Fig. 3a-3c. As seen on Fig. 3c, Δf increases when ξ decreases, which implies that the shift in resonance frequency should be larger for sample B than for sample D. However, when looking at Fig. 3a and Fig 3b, it is seen that the shift is greatest for sample D. This anomaly can be explained by the fact that the relative change in effective length due to δ is larger for the sample with the shortest centerline (sample D), resulting in a larger frequency shift.

Lastly, it is seen that the shift in resonance frequency is related to the value of both ξ and τ. The dependency of Δf on ξ can be explained by looking at Fig. 3c. In this figure, it is seen that the resonance frequency varies, although both the centerline length and resonator cross-section are the same for all four samples. This implies that the position of the fold ξ is indeed of importance when determining the effective length of a folded resonator. The dependency of Δf on τ can be explained in a similar way by comparing the experimental results for sample D (Fig. 3b) and sample G (Fig. 3c). Based on the two previous conclusions, Δf should be largest for sample D as this sample has the shortest centerline length. However, it is noticed that the shift is largest for sample G. This peculiarity can be explained by a dependence of the effective length on the resonator width b. This double dependency was already indicated by Eqn.(5)-(5b).

4.4.2 Accuracy of the proposed length correction factor

Apart from knowing how the resonance frequency changes due to a 90° fold, Eqn.(5)-(5b) also allow to calculate the eventual first resonance frequency. Being able to predict this frequency facilities the design process of real-life resonators.

The absorption curves for samples A-D are given in **Fig. 5.** Fig. 5a-5d display the data corresponding to samples A-D, respectively. The solid lines represent the analytical results for the ideal geometries with effective length correction. The dotted lines represent the analytical results for the real geometries with effective length correction, and the dashed lines represent the experimental results.

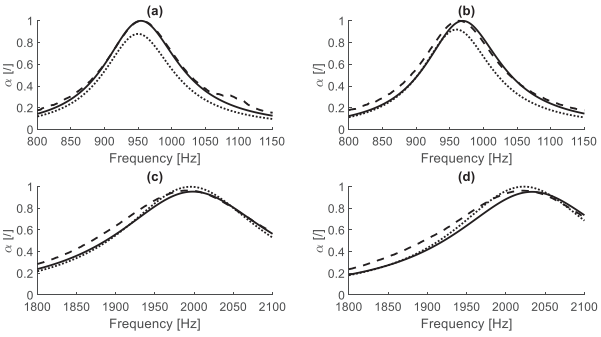

Figure 5. Overview of the analytical (ideal (−) and real (···) geometry) and experimental (---) results for samples A-D

Likewise, the absorption curves for samples E-H are given in **Fig. 6**. Fig. 6a-6d display the data corresponding to samples E-H, respectively.

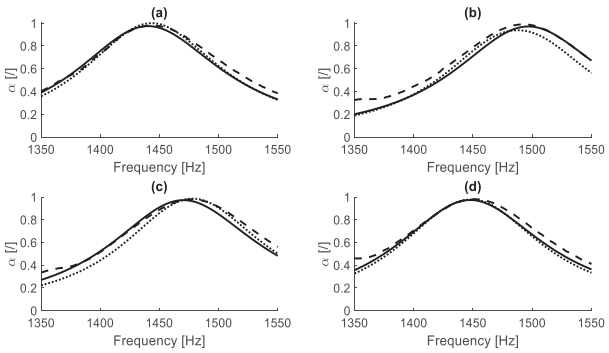

Figure 6. Overview of the analytical (ideal (−) and real (⋯) geometry) and experimental (---) results for samples E-H

An overview of the ideal, corrected and experimental resonance frequencies and achieved accuracy for all eight samples can be found in **Tab. 2.** The values in the second and third column of Tab. 2 are calculated using Eqn.(1)-(5b) and the ideal or real resonator geometry, respectively. The relative errors (columns 5-8) are calculated using the data out of the third and fourth column:

- Each value in column 5 is calculated as the relative difference between the experimental and analytical resonance frequency of that sample;
- The values in column 6 are calculated as the relative difference between the experimental result for that sample and the analytical result for the corresponding unfolded geometry (i.e. sample A, C or E);
- The values in columns 7a-8b are calculated in a similar way, now accounting for the repeatability of the test procedure (Section 4.2) - i.e. using an experimental resonance frequency that is either κ Hz smaller (columns 7a and 8a) or κ Hz greater (columns 7b and 8b) than the measured value (column 4).

From Tab. 2 and Fig. 5-6, the following can be concluded:

- The analytical predictions follow the trend of the experimental results, which implies that Eqn.(5)-(5b) indeed manage to grasp the effect of folding correctly.
- In general, it can be said that using the real dimensions (Section 4.3) allows for a more accurate prediction of the resonance frequency as compared to using the ideal geometry. When looking closer, it is seen that, on average, the absolute difference between the predicted and experimental resonance frequency is larger for samples A-D than for samples E-H. This peculiarity can most likely be attributed to the fact that the centerline lengths of the resonators of samples A-D are estimated instead of directly measured. However, further research is needed to establish this conclusion.
- When looking at the achievable level of accuracy, it is seen that using Eqn.(5)-(5b) leads to an average relative error between the predicted and actual resonance frequency of 0.20 %. When taking into account the repeatability of the measurement procedure (Section 4.2), this value increases to 0.32 %. In comparison, not using the proposed length correction factor leads to a maximum relative error of 1.18 % or, when looking at repeatability, 1.23%.

Table 2. An overview of the ideal, corrected and experimental resonance frequencies and achieved accuracy for all eight samples. (δ) indicates the use of Eqn.(5)-(5b), (-) assumes no length correction factor.

Sample	**Ideal geometry**	**Real geometry**	**Experiments**	**|% error| (δ)**	**|% error| (-)**	**|% error| repeatability (δ)**		**|% error| repeatability (-)**	
A	954 Hz	950 Hz	955 Hz	0.52	0.52	0.11	0.94	0.11	0.94
B	969 Hz	959 Hz	964 Hz	0.52	1.45	0.11	0.93	1.04	1.86
C	1998 Hz	1995 Hz	1995 Hz	0	0	0.20	0.20	0.20	0.20
D	2033 Hz	2023 Hz	2020 Hz	0.15	1.24	0.35	0.05	1.04	1.43
E	1440 Hz	1443 Hz	1444 Hz	0.07	0.07	0.21	0.34	0.21	0.34
F	1495 Hz	1487 Hz	1492 Hz	0.33	3.28	0.07	0.60	3.02	3.54
G	1470 Hz	1478 Hz	1478 Hz	0	2.37	0.27	0.27	2.10	2.63
H	1448 Hz	1450 Hz	1450 Hz	0	0.48	0.28	0.27	0.21	0.76
AVERAGE ERROR (%)				**0.20**	**1.18**	**0.32**		**1.23**	

5. CONCLUSIONS AND OUTLOOK

In this paper, the use of a correction factor to calculate the effective length of a folded resonator is experimentally validated by means of impedance tube measurements, which were performed according to the ISO 10534-2 standard.

The proposed length correction factor δ (Eqn.(5)-(5b)) was derived out of numerical simulations and is a function of both the resonator width and the distance between the center of the fold and the resonator opening. It was seen that this factor not only grasps the effect of folding correctly, but also leads to significant smaller average error between the predicted and experimental resonance frequency (0.32 %) as compared to not using a correction factor (1.23 %). Hence, it can be concluded that using the proposed correction factor is justified.

Additionally, it was noticed that using the real resonator dimensions generally leads to a more accurate prediction of the resonance frequency as compared to using the ideal dimensions. However, measuring the real dimensions and inspecting each resonator on production defects can (i) only be done post-production, (ii) is time-consuming and prone to human errors and/or (iii) requires specific techniques (e.g. optics), which are not always available. Hence, it is important that both the geometrical accuracy and possibility of defects in 3D printed parts can be estimated and accounted for during the design/modelling phase.

It should be noted that, in this work, only resonators with a rectangular cross-section have been investigated experimentally. However, since Eqn.(5)-(5b) can also be applied to slit-like resonators, experimental validation of such geometries is planned. In addition, a numerical study on the applicability of Eqn.(5)-(5b) for resonators with multiple 90° bends is ongoing. The goal of this study is two-fold: (i) check if an additional correction is needed when the distance between two consecutive bends is lower than a certain limit and (ii) determine the most efficient way of modelling the effect of multiple bends on the resonance frequency, not limited by the number of bends and their intermediate distance. Later, this formula will also be experimentally validated.

6. ACKNOWLEDGMENTS

The research of F. De Bie (fellowship no. 1S17422N) is funded by a personal grant from the Research Foundation - Flanders (FWO).

7. REFERENCES

[1] F. De Bie et al., “Quarter-wavelength acoustic metamaterials: the effect of folding on the resonance frequency”, in *Proc. of ISMA-USD 2022*, pp. 3054 – 3065, 2022.

[2] Y. Min et al. “Optimal Sound-Absorbing Structures,” *Materials Horizon*, vol. 4, pp. 673–680, 2017.

[3] Y. Wang et al. “A tunable sound-absorbing metamaterial based on coiled-up space,” *Journal of Applied Physics*, no. 123, 2018.

[4] C. Chen et al. “A low-frequency sound absorbing material with subwavelength thickness,” *Applied Physics Letter*, no. 110, 2017.

[5] A. Carvalho de Sousa et al. “On the assembly of Archimedean spiral cavities for sound absorption applications: Design, optimization and experimental validation,” *Mechanical Systems and Signal Processing*, no. 147, 2021.

[6] T. Dupont et al. “A microstructure material design for low frequency sound absorption,” *Applied Acoustics*, no. 136, pp. 86-93, 2018.

[7] Z. Zhang et al. “Optimized Metamaterial Using Quarter-wavelength Resonators for Broadband Acoustic Absorption”, in *Proc. of DAGA*, 2021.

[8] J.F. Allard and N. Atalla: *Propagation of Sound in Porous Media: Modelling Sound Absorbing Materials (2nd edition)*. City: Chichester, 2009.

[9] M. L. Munjal: *Acoustics of ducts and mufflers with application to exhaust and ventilation system design*. City: Calgary, 1987.

[10] B.E. Anderson, “Understanding radiation impedance through animations”, in *Proc. of Meetings on Acoustics*, vol. 33, 2020.

[11] L. Jaouen and F. Chevillotte, “Length Correction of 2D Discontinuities or Perforations at Large Wavelengths and for Linear Acoustics,” *Acta Acustica united with Acustica*, no. 136, pp. 243-250, 2018.

[12] G.T. Zielinski et al., “Sound absorption of plates with micro-slits backed with air cavities: analytical estimations, numerical calculations and experimental validations,” *Applied Acoustics*, no. 146, pp. 261-279, 2019.

[13] “Intent profiles in Ultimaker Cura” (2022). Online: https://support.makerbot.com/s/article/1667411132905

[14] ISO 5725-6 standard, “Accuracy (trueness and precision) of measurement methods and results — Part 6: Use in practice of accuracy values”, 1994